Available online at www.sciencedirect.com
ScienceDirect
Journal of Computational Physics 227 (2007) 1–11
JOURNAL OF COMPUTATIONAL PHYSICS
www.elsevier.com/locate/jcp

Short Note

On the characteristics-based ACM for incompressible flows

Xiaohui Su, Yong Zhao *, Xiaoyang Huang

School of Mechanical and Aerospace Engineering, Nanyang Technological University, Nanyang Avenue, Singapore 639798, Republic of Singapore

Received 19 April 2007; received in revised form 2 August 2007; accepted 8 August 2007
Available online 25 August 2007

Abstract

In this paper, the revised characteristics-based (CB) method for incompressible flows recently derived by Neofytou [P. Neofytou, Revision of the characteristic-based scheme for incompressible flows, J. Comput. Phys. 222 (2007) 475–484] has been further investigated. We have derived all the formulas for pressure and velocities from this revised CB method, which is based on the artificial compressibility method (ACM) [A.J. Chorin, A numerical solution for solving incompressible viscous flow problems, J. Comput. Phys. 2 (1967) 12]. Then we analyze the formulations of the original CB method [D. Drikakis, P.A. Govatsos, D.E. Papatonis, A characteristic based method for incompressible flows, Int. J. Numer. Meth. Fluids 19 (1994) 667–685; E. Shapiro, D. Drikakis, Non-conservative and conservative formulations of characteristics numerical reconstructions for incompressible flows, Int. J. Numer. Meth. Eng. 66 (2006) 1466–1482; D. Drikakis, P.K. Smolarkiewicz, On spurious vortical structures, J. Comput. Phys. 172 (2001) 309–325; F. Mallinger, D. Drikakis, Instability in three-dimensional, unsteady stenotic flows, Int. J. Heat Fluid Flow 23 (2002) 657–663; E. Shapiro, D. Drikakis, Artificial compressibility, characteristics-based schemes for variable density, incompressible, multi-species flows. Parts I. Derivation of different formulations and constant density limit, J. Comput. Phys. 210 (2005) 584–607; Y. Zhao, B. Zhang, A high-order characteristics upwind FV method for incompressible flow and heat transfer simulation on unstructured grids, Comput. Meth. Appl. Mech. Eng. 190 (5–7) (2000) 733–756] to investigate their consistency with the governing flow equations after convergence has been achieved. Furthermore we have implemented both formulations in an unstructured-grid finite volume solver [Y. Zhao, B. Zhang, A high-order characteristics upwind FV method for incompressible flow and heat transfer simulation on unstructured grids, Comput. Meth. Appl. Mech. Eng. 190 (5–7) (2000) 733–756]. Detailed numerical experiments show that both methods give almost identical solutions and convergence rates. Both can generate solutions which agree well with published results and experimental measurements. We thus conclude that both methods, being upwind schemes designed for the ACM, have the same performances in terms of accuracy and convergence speed, even though the revised method is more complex with less stringent assumptions made, while the original CB method is simpler due to the use of extra simplifying assumptions.

Keywords: Characteristics-based method; Artificial compressibility method (ACM); Compatibility equations; Incompressible flows

* Corresponding author. Tel.: +65 67904545; fax: +65 792 4062.
E-mail address: myzhao@ntu.edu.sg (Y. Zhao).

0021-9991/$ - see front matter © 2007 Elsevier Inc. All rights reserved.
doi:10.1016/j.jcp.2007.08.009

1. Introduction

The original CB method for the ACM has been proposed by Drikakis et al. [3] as an upwind scheme on boundary-fitted structured grids to compute incompressible flows. Afterwards, the method has been developed and applied by Shipiro and Drikakis [4] on non-conservative and conservative formulations of characteristics numerical reconstructions for incompressible flows; Drikakis and Smolarkiewicz [5] on spurious vertical structure; Mallinger and Drikakis [6] on the instability in 3D unsteady stenotic flows; and Shipiro and Drikakis [7] for variable density, incompressible, multi-species flows. At the same time, Zhao et al. [8] have developed a general higher-order finite-volume unstructured grid method for incompressible flows based on the CB method and ACM. The above references show the CB scheme has been successfully used in a number of applications.

Recently Neofytou [1] proposed revisions in the derivation of the compatibility equations which are used to derive the CB formulas for the calculations of the primitive flow valuables. It is found that over simplifying assumptions have been made in the original CB scheme for the derivation of the compatibility equations for $\lambda = \lambda^0$ in 2D and 3D [1].

In this paper, the revised compatibility equations have been further investigated. It is released that both the original and new CB methods are derived based on the ACM with the introduction of pseudo-time dependent terms. Their primary purposes are to introduce stable upwinding to help the solution of the ACM converge to physically meaningful one. Through detailed analysis of the original CB method, we also find that after converged solution is achieved, its formulations are consistent with the conservation laws. Furthermore we have derived the formulations for calculating the primitive flow variables based on the revised CB method, which have not been given in [1]. The original and revised methods are then implemented into an unstructured-grid solver developed by Zhao et al. [8]. Numerical experiments have been conducted to compare the accuracy and convergence speed of the two methods. It is found that they are basically identical in their performances although they are based on different assumptions and have different levels of complexities.

2. The original CB method

The Euler equation modified by Chorin's ACM [2] are rewritten in partial differential form in a Cartesian co-ordinate system for the derivation of the CB method:

$$\frac{\partial p}{\partial \tau} + \beta \frac{\partial u_i}{\partial x_i} = 0 \tag{1}$$

$$\frac{\partial u_i}{\partial \tau} + u_j \frac{\partial u_i}{\partial x_j} + u_i \frac{\partial u_j}{\partial x_j} + \frac{\partial p}{\partial x_i} = 0 \tag{2}$$

where subscripts i and j equal 1, 2 and 3, representing the co-ordinates x, y and z. If we introduce finite-volume unstructured grid method [8] for the numerical solution of the equations, we can construct control volumes that surround every mesh node and store flow valuables at these nodes using the vertex-centered scheme. Suppose that ξ is a new co-ordinate which is in the direction of the outward normal vector of the surface of a control volume that surrounds a particular vertex. For arbitrary unstructured meshes, the preceding equations can then be transformed into

$$\frac{\partial p}{\partial \tau} + \beta \frac{\partial u_j}{\partial \xi} \xi_{x_j} = 0 \tag{3}$$

$$\frac{\partial u_i}{\partial \tau} + u_j \frac{\partial u_i}{\partial \xi} \xi_{x_j} + u_i \frac{\partial u_j}{\partial \xi} \xi_{x_j} + \frac{\partial p}{\partial \xi} \xi_{x_i} = 0 \tag{4}$$

where $\xi_{x_i} = \frac{\partial \xi}{\partial x_i}$ and $\xi_{x_j} = \frac{\partial \xi}{\partial x_j}$.

In the τ–ξ space as shown in Fig. 1, flow variable vector $\mathbf{W}$, where $W = \{p, u, v\}^{\mathrm{T}}$, at pseudo time level $m+1$ can be calculated along a characteristics, k, using a Taylor series expansion and the initial value at pseudo time level m ($\mathbf{W}_k$):

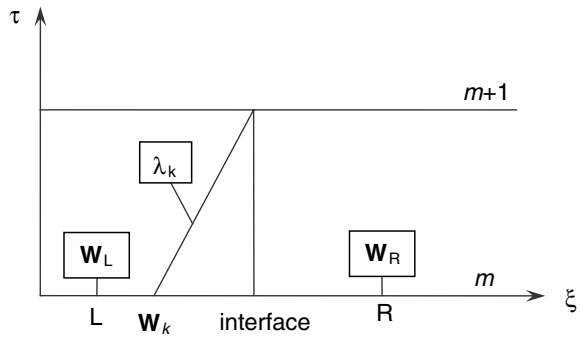

Fig. 1. τ–ξ Co-ordinate.

$$\mathbf{W} = \mathbf{W}_k + \mathbf{W}_\xi \xi_\tau \Delta\tau + \mathbf{W}_\tau \Delta\tau \tag{5}$$

and

$$\mathbf{W}_\tau = \frac{\mathbf{W} - \mathbf{W}_k}{\Delta\tau} - \mathbf{W}_\xi \xi_\tau \tag{6}$$

A wave speed, λ_k, is introduced as

$$\xi_\tau = \lambda_k \sqrt{\xi_{x_i} \xi_{x_i}}$$

and the unit normal vector components are

$$n_{x_j} = \frac{\xi_{x_j}}{\sqrt{\xi_{x_i} \xi_{x_i}}}$$

Substituting components of $\mathbf{W}_\tau$ into Eqs. (3) and (4), we have

$$\frac{1}{\sqrt{\xi_{x_i} \xi_{x_i}}} \frac{(p - p_k)}{\Delta\tau} - p_\xi \lambda_k + \beta(u_\xi n_x + v_\xi n_y) = 0 \tag{7}$$

$$\frac{1}{\sqrt{\xi_{x_i} \xi_{x_i}}} \frac{(u - u_k)}{\Delta\tau} - u_\xi(\lambda_0 - \lambda_k) + u(u_\xi n_x + v_\xi n_y) + p_\xi n_x = 0 \tag{8}$$

$$\frac{1}{\sqrt{\xi_{x_j} \xi_{x_j}}} \frac{(v - v_k)}{\Delta\tau} - v_\xi(\lambda_0 - \lambda_k) + v(u_\xi n_x + v_\xi n_y) + p_\xi n_y = 0 \tag{9}$$

where λ_0 is the fluid velocity in normal direction:

$$\lambda_0 = u n_x + v n_y$$

In order to derive the compatibility equations, spatial derivatives, such as u_ξ, v_ξ, and p_ξ have to be eliminated from the preceding equations. Following the approaches in [3,9] for both compressible and incompressible flow equations, each of the preceding three equations is multiplied by an arbitrary variable and all the resulting equations are summed to form a new equation as follows:

$$\frac{1}{\Delta\tau \sqrt{\xi_{x_j} \xi_{x_j}}} A - p_\xi B + u_\xi C + v_\xi D = 0 \tag{10}$$

where

$$\begin{aligned} A &= a(p - p_k) + b(u - u_k) + c(v - v_k) \\ B &= -a\lambda_k + b n_x + c n_y \\ C &= a n_x \beta + b(\lambda_0 - \lambda_k + u n_x) + c v n_x \\ D &= a n_y \beta + b u n_y + c(\lambda_0 - \lambda_k + v n_y) \end{aligned} \tag{11}$$

a, b, and c are the arbitrary variables used to multiply the equations. We set the coefficients of the partial spatial derivatives to be zero, i.e., A, B, C, and D are zero:

$$A = a(p - p_k) + b(u - u_k) + c(v - v_k) = 0 \tag{12}$$

$$B = -a\lambda_k + bn_x + cn_y = 0 \tag{13}$$

$$C = an_x\beta + b(\lambda_0 - \lambda_k + un_x) + cvn_x = 0 \tag{14}$$

$$D = an_y\beta + bun_y + c(\lambda_0 - \lambda_k + vn_y) = 0 \tag{15}$$

Eqs. (13)–(15) constitute a linear system $\Phi X = 0$ with $X = \{a, b, c\}$. Variables a, b, and c are generally non-zero. Thus the system of equations has non-trivial solution. This means that $\det(\Phi) = 0$, and then the following λ_k values can be derived:

$$\lambda_0 = un_x + vn_y$$

$$\lambda_1 = \lambda_0 + \sqrt{(\lambda_0)^2 + \beta} = \lambda_0 + C$$

$$\lambda_2 = \lambda_0 - \sqrt{(\lambda_0)^2 + \beta} = \lambda_0 - C$$

For each λ_k, characteristic equations can be derived from Eqs. (12)–(15). For example, for $\lambda_k = \lambda_0$, we have

$$a = \frac{bn_x + cn_y}{\lambda_0} \tag{16}$$

Substituting this into Eq. (12), we obtain

$$\frac{bn_x + cn_y}{\lambda_0}(p - p_0) + b(u - u_0) + c(v - v_0) = 0$$

that is

$$b[n_x(p - p_0) + \lambda_0(u - u_0)] + c[n_y(p - p_0) + \lambda_0(v - v_0)] = 0 \tag{17}$$

For any b and c, the preceding equations are always satisfied. All the terms in square brackets are set to zero. As a result, we have,

$$(u - u_0)n_y - (v - v_0)n_x = 0 \tag{18}$$

The above equation is equivalent to the following condition:

$$U_t = (U_t)_0$$

i.e. the tangent velocity is assumed to be constant near the control volume surface, which is a reasonable assumption for the extension of a 1D method to multi-dimensional ones with arbitrary unstructured meshes. For $\lambda = \lambda_1$,

$$p - p_1 = -\lambda_1[(u - u_1)n_x + (v - v_1)n_y] \tag{19}$$

For $\lambda = \lambda_2$,

$$p - p_2 = -\lambda_2[(u - u_2)n_x + (v - v_2)n_y] \tag{20}$$

Finally, u, v and p are determined using the preceding characteristics equations (18)–(20):

$$u = fn_x + n_y(u_0n_y - v_0n_x) \tag{21}$$

$$v = fn_y + n_x(v_0n_x - u_0n_y) \tag{22}$$

$$p = \frac{\lambda_1[p_2 + \lambda_2(u_2n_x + v_2n_y)] - \lambda_2[p_1 + \lambda_1(u_1n_x + v_1n_y)]}{2C} \tag{23}$$

where

$$C = \sqrt{(\lambda_0)^2 + \beta}$$

$$f = \frac{1}{2C}[(p_1 - p_2) + n_x(\lambda_1 u_1 - \lambda_2 u_2) + n_y(\lambda_1 v_1 - \lambda_2 v_2)]$$

Flow quantities at $m+1$ pseudo time level obtained from the preceding equations on the characteristics are then used to calculate convection fluxes at the control volume interface. Those on different characteristics at m pseudo time level are approximately evaluated by an upwind scheme using the signs of the characteristics as suggested by Drikakis et al. [3].

$$\mathbf{W}_j = \frac{1}{2}[(1 + \mathrm{sign}(\lambda_j))\mathbf{W}_\mathrm{L} + (1 - \mathrm{sign}(\lambda_j))\mathbf{W}_\mathrm{R}]$$

where $\mathbf{W}_\mathrm{L}$ and $\mathbf{W}_\mathrm{R}$ are obtained by the upwind-biased interpolation.

The advantages of the characteristics scheme are: (i) stable solution without adding artificial viscosity; (ii) less sensitive to grid orientation because flow signals are propagated along characteristics.

3. Theoretical analysis of the original CB method

It should be noted that the ACM method does not produce physically meaningful results before the convergence of the solution, i.e., the disappearance of the pseudo-time dependent terms. After the convergence, Eq. [3] becomes

$$\frac{\partial U_n}{\partial \xi} = 0 \tag{24}$$

And Eq. (4) can be reformulated as

$$\frac{\partial U_n^2}{\partial \xi} + \frac{\partial p}{\partial \xi} = 0 \tag{25}$$

Integrating the above two equations along ξ for all the characteristics (now τ has disappeared), we have

$$U_n = (U_n)_k \tag{26}$$

$$U_n^2 + p = (U_n^2 + p)_k \tag{27}$$

Based on Eqs. (26) and (27), we also have

$$P = P_k \tag{28}$$

Therefore it is noted that when convergence is achieved, all the state vectors containing the primitive flow valuables that are linked to the state on the interface through all the characteristics converge to the same state, which is the state on the interface itself:

$$\mathbf{W} = \mathbf{W}_k \tag{29}$$

We now analyze the relation between the original CB and the convergent equations in Eqs. (26)–(29). From Eqs. (21) and (22), we can derive

$$U_n = \frac{p_1 - p_2 + U_n[(U_n)_1 - (U_n)_2] + [(U_n)_1 + (U_n)_2]\sqrt{(U_n)^2 + \beta}}{2\sqrt{(U_n)^2 + \beta}} \tag{30}$$

And from Eq. (23) the following is obtained:

$$p = \frac{U_n(p_2 - p_1) - \beta[(U_n)_2 - (U_n)_1] + (p_2 + p_1)\sqrt{(U_n)^2 + \beta}}{2\sqrt{(U_n)^2 + \beta}} \tag{31}$$

It is obvious that after convergence is achieved, Eqs. (30) and (31) become the same as Eqs. (26)–(29). This means that the original CB method leads to convergent solutions that are consistent with the conservation laws.

4. The revised CB method

Neofytou [1] proposes a revision to the first compatibility equation, Eq. (18), based on the argument that in Eq. (17) b and c are related. He thought that setting the terms in the square brackets in Eq. (17) to zero is too stringent a condition. If Eq. (16) is substituted into Eq. (14) then

$$b = -c\frac{\beta n_y + \lambda_0 v}{\beta n_x + \lambda_0 u} \tag{32}$$

Substituting Eq. (32) into Eq. (16) yields

$$a = c\beta\frac{un_y - vn_x}{\beta n_x + \lambda_0 u} \tag{33}$$

By substituting Eqs. (32) and (33) into Eq. (13) we have

$$(p - p_0)(un_y - vn_x) - (u - u_0)(\beta n_y + \lambda_0 v) + (v - v_0)(\beta n_x + \lambda_0 u) = 0 \tag{34}$$

Thus Neofytou [1] considers Eq. (34), not Eq. (18), as the compatibility equation for $\lambda = \lambda_0$. For $\lambda = \lambda_1$ and $\lambda = \lambda_2$, the compatibility equations are the same as Eqs. (19) and (20), respectively, and are obtained following a procedure similar to the derivation of Eqs. (34). Details are given below. Here Eq. (13) $\times n_y$ − Eq. (14) $\times n_x$ leads to

$$bn_y(\lambda_0 - \lambda_k) + cn_x(\lambda_k - \lambda_0) = 0$$

i.e.

$$b = \frac{cn_x}{n_y} \tag{35}$$

By substituting Eq. (35) into Eq. (13) we have

$$a = \frac{c}{n_y\lambda_k} \tag{36}$$

If we substitute Eqs. (35) and (36) into Eq. (12), then the following is obtained:

$$\frac{c}{n_y\lambda_k}(p - p_k) + \frac{cn_x}{n_y}(u - u_k) + c(v - v_k) = 0$$

Thus Eqs. (19) and (20) are thus derived as follows:

$$(p - p_k) + \lambda_k[n_x(u - u_k) + n_y(v - v_k)] = 0$$

here $k = 1$ and 2.

Therefore Eqs. (34), (19) and (20) consist of the revised compatibility equations, which can be used to derive expressions for primitive values p, u and v as functions of their characteristic values.

5. Primitive flow variables based on the revised CB method

Here we use a mathematics tool, Maple, to help derive the expressions for the primitive valuables, such as p, u and v from the revised compatibility equations. After lengthy manual simplifications, the final equations are obtained as follows:

$$p = \frac{\lambda_1\lambda_2[(u_2n_x + v_2n_y) - (u_1n_x + v_1n_y)] - \lambda_2 p_1 + \lambda_1 p_2}{\lambda_1 - \lambda_2} \tag{37}$$

$$u = \frac{u_a}{u_b} \tag{38}$$

where

$$
\begin{aligned}
u_a =& [\lambda_1(n_x u_1 + n_y v_1) - \lambda_2(n_x u_2 + n_y v_2)]\{n_x(\lambda_2 p_1 - \lambda_1 p_2) + (\lambda_1 - \lambda_2)[\lambda_0 u_0 + n_x(p_0 + \beta)] \\
&+ n_x\lambda_1\lambda_2[(n_x u_1 + n_y v_1) - (n_x u_2 + n_y v_2)]\} + n_x\lambda_1\lambda_2(p_1 - p_2)[(n_x u_1 + n_y v_1) - (n_x u_2 + n_y v_2)] \\
&+ (\lambda_2 - \lambda_1)\{n_y\beta(\lambda_2 - \lambda_1)(n_y u_0 - n_x v_0) + (p_2 - p_1)[\lambda_0 u_0 + n_x(p_0 + \beta)]\} + n_x(p_2 - p_1)(\lambda_1 p_2 - \lambda_2 p_1)
\end{aligned}
$$

and

$$
\begin{aligned}
u_b &= (\lambda_1 - \lambda_2)\{\lambda_2 p_1 - \lambda_1 p_2 + \lambda_1\lambda_2[(n_x u_1 + n_y v_1) - (n_x u_2 + n_y v_2)] + (\lambda_1 - \lambda_2)[p_0 + \beta + \lambda_0(n_x u_0 + n_y v_0)]\} \\
v &= \frac{v_a}{v_b}
\end{aligned}
\tag{39}
$$

where

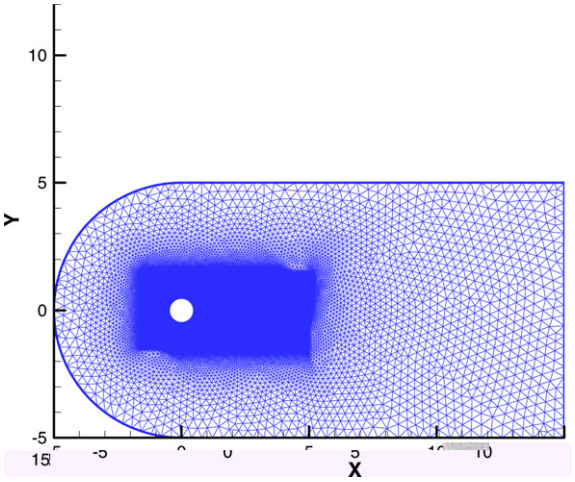

Fig. 2. Fluid mesh for stationary circular cylinder flow at $Re = 40$.

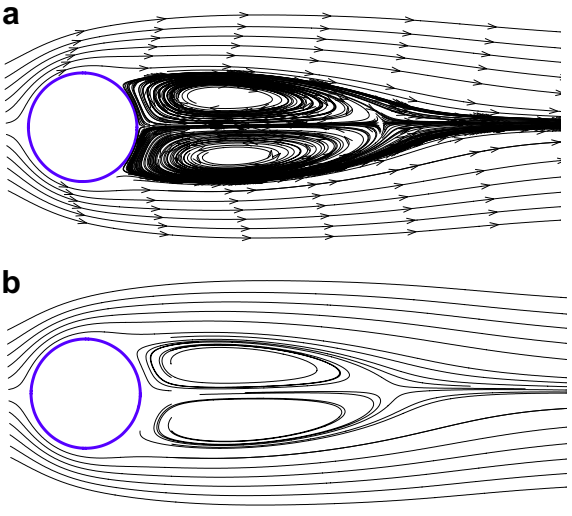

$$
\begin{aligned}
v_a =& (n_x u_1 + n_y v_1)\{\lambda_1\lambda_1\lambda_2 n_y[(n_x u_1 + n_y v_1) - (n_x u_2 + n_y v_2)] + \lambda_0\lambda_1(\lambda_2 - \lambda_1)v_0 + \lambda_1\lambda_1 n_y(p_0 - \beta - p_2) \\
&+\lambda_1\lambda_2 n_y[2p_1 - p_2 - p_0 + \beta]\} + (n_x u_2 + n_y v_2)\{\lambda_1\lambda_2\lambda_2 n_y[(n_x u_2 + n_y v_2) - (n_x u_1 + n_y v_1)] \\
&+\lambda_0\lambda_1(\lambda_1 - \lambda_2)v_0 + \lambda_2\lambda_2 n_y(p_0 - \beta - p_1) + \lambda_1\lambda_2 n_y[2p_2 - p_1 - p_0 + \beta]\} \\
&+ n_x\beta(\lambda_2 - \lambda_1)(\lambda_2 - \lambda_1)(n_y u_0 - n_x v_0) + \lambda_0 v_0[(\lambda_2 - \lambda_1)(p_1 - p_2)] \\
&+ n_y(p_2 - p_1)[\lambda_1 p_2 - \lambda_2 p_1 + (p_0 - \beta)(\lambda_2 - \lambda_1)]
\end{aligned}
$$

and

$$
\begin{aligned}
v_b =& (\lambda_2 - \lambda_1)\{-\lambda_0[(\lambda_2 - \lambda_1)(n_x u_0 + n_y v_0)] - \lambda_1\lambda_2[(n_x u_1 + n_y v_1) - (n_x u_2 + n_y v_2)] + [(\lambda_2 - \lambda_1)(p_0 - \beta) \\
&+\lambda_1 p_2 - \lambda_2 p_1]\}
\end{aligned}
$$

Table 1
Length of separation bubbles behind cylinder ($Re = 40$)

Methods	S/D
Experiment [10]	2.35
Original CB method	2.31
Revised CB method	2.31

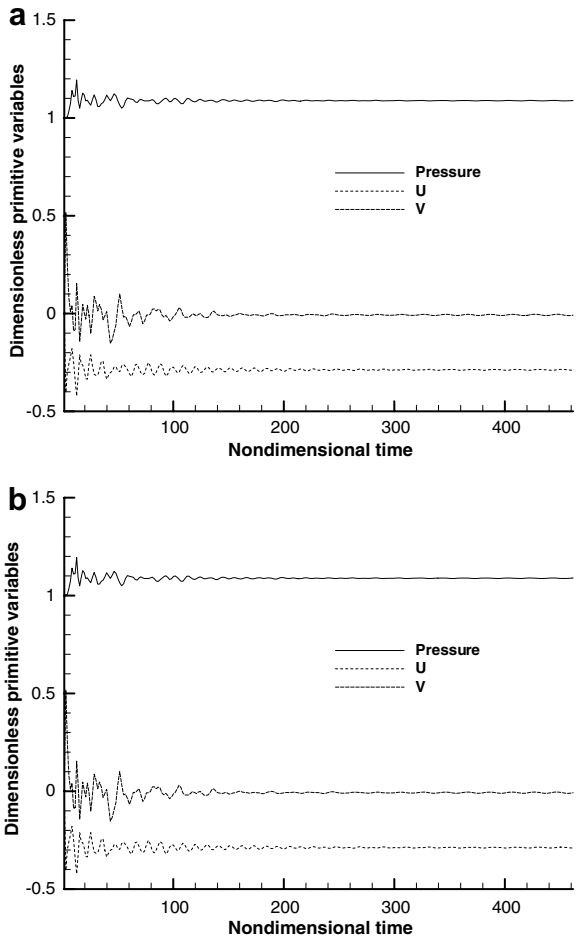

Fig. 4. Time histories of primitive variables on a control volume interface: (a) the original CB method; (b) revised CB method.

6. Numerical investigation of the two methods

In this section, numerical experiments are conducted to investigate the performances of the original CB and revised CB methods. In order to generate comparable results, these two methods are implemented into the same solver [8] and the same mesh is used to simulate the same problem to generate results for comparison. The test case is laminar flow over a circular cylinder at Reynolds number equal to 40. The fluid mesh consists of 67,702 nodes and 134,625 elements (see Fig. 2). In both cases the number of pseudo sub-iterations per time step is set to 200 and CFL is set to 3.5. The streamlines around the cylinder obtained using the original CB method are compared with those of the revised CB method in Fig. 3, which are almost identical. Table 1 gives a comparison of the aspect ratios calculated by both methods (separation bubble length, S over cylinder diameter, D) with the experimental results obtained by Nishioka and Sato [10]. Both results agree well each other and the experimental ones.

In order to further investigate the differences in results generated by the two methods, the values of primitive variables on a particular control volume interface are recorded in Fig. 4. Moreover, their residuals histories versus CPU time are plotted in Fig. 5 and the lift and drag coefficients versus non-dimensional time are plotted in Fig. 6. Fig. 5 indicated that the convergent rate of original method is bit of faster than that of revised method. Authors thought the mainly reason is the expressions of primitive variables, p, u and v for the original method Eqs. (21)–(23), are much simpler than those for the revised one Eqs. (37)–(39). Table 2 gives a comparison of drag coefficient calculated by both methods with other published results, which again

Table 2
The comparison of drag coefficient ($Re = 40$)

Methods	CD
Takami and Keller [11]	1.5359
Dennis and Chang [12]	1.522
Nieuwstadt and Keller [13]	1.550
Original CB method	1.5303
Revised CB method	1.5301

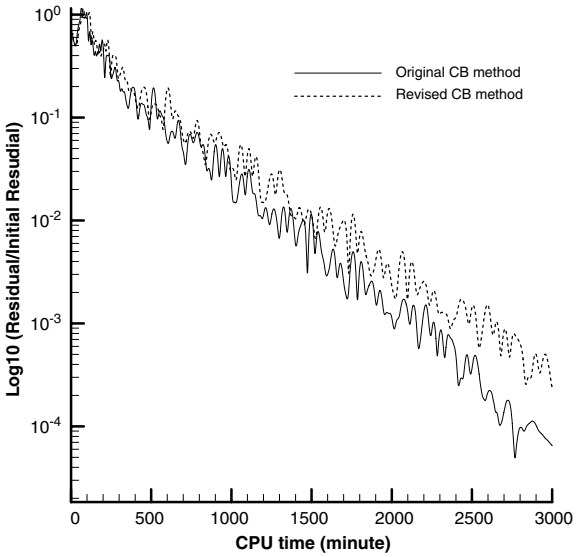

Fig. 5. Residuals versus CPU time (in min) for original CB method (solid line) and revised CB method (dot line).

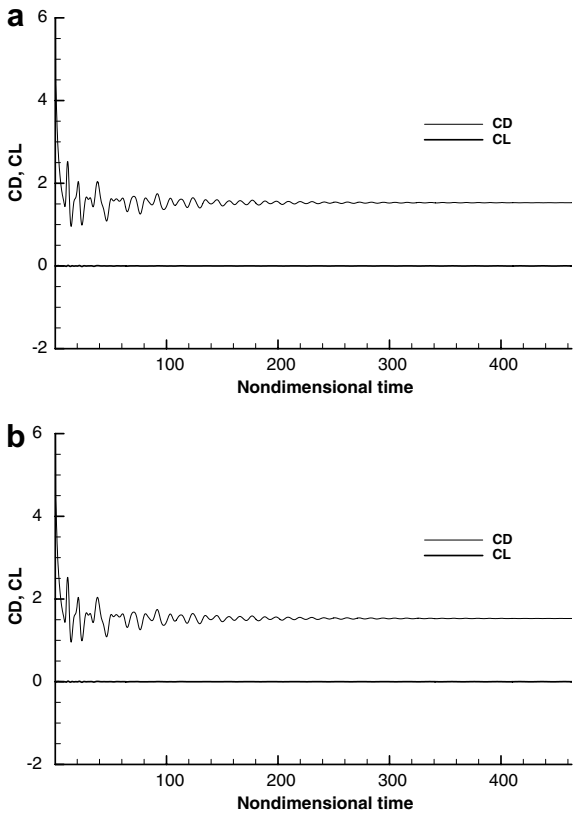

Fig. 6. Lift (CL) and drag (CD) coefficients versus non-dimensional time for flow over a stationary cylinder ($Re = 40$): (a) the original CB method; (b) revised CB method.

shows excellent agreement. The computational results in Figs. 4–6 show almost identical predictions and convergence rates for the two methods, with the original one being slightly faster in convergence speed. The solvers are run on a personal computer using Intel Xeon dual CPU with a clock speed of 2.8 GHz.

7. Conclusions

In this paper, the revised compatibility equations derived by Neofytou [1] have been investigated. Furthermore a theoretical study of the original CB method has also been undertaken to analyze its compatibility with the converged equations of the ACM, which are the conservation laws. The mathematical expressions for primitive flow variables based on the revised CB method are derived and incorporated into an unstructured-grid flow solver [4], together with the original CB formulations. Numerical experiments are then conducted to compare the performances of the two methods, as well as to validate their results. We can thus conclude that: (1) the two methods, being based on the ACM, do not have physical meaning, but they are only used as upwind schemes to facilitate the convergence of the modified equations of the ACM to the conservation equations, from which the final converged numerical solutions are obtained; (2) both methods can generate the same converged solutions accurately, which agree well with experimental measurements; (3) both have the same convergence speeds using the same mesh for the same test case; (4) the revised CB method is more complex with less stringent assumptions made, while the original CB method is simpler due to the use of more simplifying assumptions, which are, nonetheless, found to be consistent with the converged equations, i.e., the conservation laws.

References

[1] P. Neofytou, Revision of the characteristic-based scheme for incompressible flows, J. Comput. Phys. 222 (2007) 475–484.
[2] A.J. Chorin, A numerical solution for solving incompressible viscous flow problems, J. Comput. Phys. 2 (1967) 12.
[3] D. Drikakis, P.A. Govatsos, D.E. Papatonis, A characteristic based method for incompressible flows, Int. J. Numer. Meth. Fluids 19 (1994) 667–685.
[4] E. Shapiro, D. Drikakis, Non-conservative and conservative formulations of characteristics numerical reconstructions for incompressible flows, Int. J. Numer. Meth. Eng. 66 (2006) 1466–1482.
[5] D. Drikakis, P.K. Smolarkiewicz, On spurious vortical structures, J. Comput. Phys. 172 (2001) 309–325.
[6] F. Mallinger, D. Drikakis, Instability in, three-dimensional, unsteady stenotic flows, Int. J. Heat Fluid Flow 23 (2002) 657–663.
[7] E. Shapiro, D. Drikakis, Artificial compressibility, characteristics-based schemes for variable density, incompressible, multi-species flows. Parts I. Derivation of different formulations and constant density limit, J. Comput. Phys. 210 (2005) 584–607.
[8] Y. Zhao, B. Zhang, A high-order characteristics upwind FV method for incompressible flow and heat transfer simulation on unstructured grids, Comput. Meth. Appl. Mech. Eng. 190 (5–7) (2000) 733–756.
[9] A. Eberle, 3D Euler calculations using characteristic flux extrapolation, AIAA Paper 85-0119, 1985.
[10] M. Nishioka, H. Sato, Mechanism of determination of the shedding frequency of vortices behind a cylinder at low Reynolds numbers, J. Fluid Mech. 89 (1978) 49–60.
[11] H. Takami, H.B. Keller, Steady two-dimensional viscous flow of an incompressible fluid past a circular cylinder, Phys. Fluids Suppl. II 12 (1969) 51–56.
[12] S.C.R. Dennis, G.Z. Chang, Numerical solutions for steady flow past a circular cylinder at Reynolds numbers up to 100, J. Fluid Mech. 42 (1970) 471–489.
[13] F. Nieuwstadt, H.B. Keller, Viscous flow past circular cylinders, Comput. Fluids 1 (1973) 59–71.